SERBIAN JOURNAL OF ELECTRICAL ENGINEERING
Vol. 20, No. 3, October 2023, 301-314

UDC: 621.3.049.77:66.017/.018 **DOI: https://doi.org/10.2298/SJEE2303301A**

Modeling and Analyzing Coupling Noise Effect of Cu-Carbon Nanotube Composite Through-Silicon Vias Interconnects Using NILT Based

Khaoula Ait Belaid[1], Hassan Belahrach[1,2], Hassan Ayad[1], Fatima Ez-Zaki[1]

Abstract: In the modern field of microelectronics, the performance of interconnects tends to decrease as the technology node advances. Therefore, Cu-CNT composite TSV interconnects are utilized due to their favorable performance. In this article, Cu-CNT composite TSV interconnects have been studied. The objective of this work was to propose an accurate method for calculating time domain coupling noise in 3D structures based on Cu-CNT composite TSVs. The equivalent lumped element circuit, the NILT method, and the T-matrix were exploited. Throughout the study, the influence of geometric parameters, temperature, and CNT filling ratio were examined. The proposed method has been validated using PSpice results. The obtained results have shown good performance and accuracy. The average percentage error observed is less than 1 %.

Keywords: 3D structures, TSV, Cu-CNT composite, NILT method, T-matrix.

1 Introduction

Over the past decade, planar integrated circuits have faced numerous limitations, particularly with the demand for miniaturized, high performance and high-speed nanoelectronics systems. As a result, Three-Dimensional Integrated Circuits (3D-ICs) based on Through-Silicon Vias (TSVs) are used. A chip consisting of multiple stacked dies is referred to as a 3D-IC. TSVs, also known as 3D/ vertical interconnects, are utilized to electrically connect the vertically stacked dies. Using TSVs is a decisive technique in the development of 3D-ICs. They provide short interconnect length, large bandwidth, and small power consumption [1 – 5]. The selection of filler material used in the TSV has a significant impact on the development of a 3D integrated system. Because of its excellent electrical, thermal conductivity, and chemical stability, copper (Cu) has long been deemed a common on-chip interconnect material. However, despite

[1]Laboratory of Electrical Systems, Energy Efficiency, and Telecommunications, Cadi Ayyad University, Marrakesh 40000, Morocco.
[2]Electrical Engineering Department, Royal School of Aeronautics, Marrakesh 40000, Morocco;
E-mails: khaoula.aitbelaid@ced.uca.ma, belahrach@yahoo.fr, ayad.ha@gmail.com, ftimaezzaki@gmail.com

being utilized as a filler material by several researchers, copper exhibits certain drawbacks over time. These include a significant increase in resistivity caused by enhanced grain boundary diffusion, surface diffusion, and the presence of highly diffusive barrier layers. However, with the continued miniaturizing of 3D structures, the reliability of Cu TSVs has become a significant concern, and the use of copper will be limited beyond some technologies. In fact, high-speed signals, device size reduction, crosstalk effect, distortion, and signal delay become the main factors affecting the performance of high-speed systems. Which confirmed that interconnects greatly affect the performance of nanoelectronics systems. These restrictions can be addressed by CNTs due to their increased mechanical and thermal durability, and conductivity. Furthermore, a bundle of CNT conducts current parallelly, that can reduce the resistive parasitic, consequently, propagation delay. Another alternative for replacing copper interconnects is graphene [6, 7] which shares similar physical and electrical properties with CNTs but offers advantages in terms of ease of fabrication. Additionally, composite- based CNTs are supposed to substitute copper interconnects in the near future [8].

To manage the issue of CU TSV's reliability, Carbon Nanotube (CNT) has been exploited to be used as a filling conductive material for TSV, because of its thermal and electrical properties [9 – 11]. Numerous papers have discussed and examined CNT TSVs electrical performance. They have demonstrated that CNT TSVs have an excellent performance over Cu ones. The advantages of CNT are particularly notable in nanometer-scale applications. At such scales, the Cu's electrical conductivity decreases because of the increase of the grain and surface boundary scattering. However, it remains challenging to conclusively prove that the CNT TSV performs better than its Cu counter on a larger scale [12 – 14].

In recent times, a Cu-CNT composite has been proposed and built for 3D structures to obtain high reliability [15]. This type of interconnect offers improved electromigration resistance while maintaining reduced conductivity [16]. The Cu-CNT composite provides a practical technique for interconnect fabrication and allows a better trade-off between reliability and performance. Furthermore, a comparison of crosstalk noise in coupled Cu and Cu-CNT interconnect structures reveals that interconnects based on Cu-CNT demonstrate better immunity to crosstalk [16]. However, certain challenges remain unresolved.

In [17, 18] the authors present an accurate and time efficient model for analyzing crosstalk noise in coupled interconnects within large-scale integration. All these models are based on Finite-Difference Time Domain (FDTD). By utilizing the proposed model, a comprehensive analysis of crosstalk in the time domain is performed, and the results demonstrate good agreement with the used simulator (HSPICE). Indeed, the aim objective of our work is to propose an

alternative analytical technique for modeling crosstalk effects and analyzing them in the time domain, considering various parameters. The analysis encompasses all possible process variations studied in [19].

The time domain performance of the Cu-CNT composite is successfully evaluated in this work. The objective is to calculate coupling noise in 3D-ICs in the time domain. Transition effects are best observed in the time domain, therefore, to analyze them, it is mandatory to obtain the waveforms of these coupling disturbances in the time domain. Noise coupling in the time-domain is obtained using the chain matrices and NILT method. The analysis is performed based on various parameters. The main sections of the document are organized as follows: the second part presents the equivalent circuit model of a pair of Cu-CNT composite TSVs, followed by a concise summary of NILT. Subsequently, the results and analysis are presented, and finally, the article concludes.

2 Cu-CNT Composite TSV model

Fig. 1 presents the conceptual view of a pair of Cu-CNT Composite TSVs. The schematic model consists of a signal and ground Cu-CNT composite TSV. The ground TSV is necessary, it presents a path of the current return. The schematic, with its equivalent circuit model of this conceptual view, is given in Fig. 2.

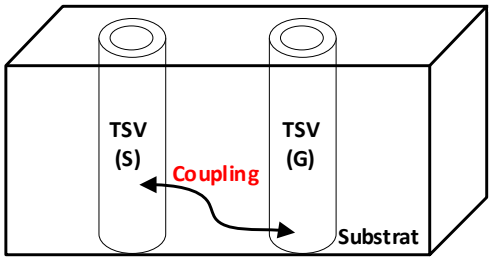

Fig. 1 – *The conceptual view of a pair of Cu-CNT Composite TSVs.*

In Fig. 2, r_{via} and h_{via} present the radius and height of the TSV, t_{ox} is the oxide thickness, t_{dep} is the depletion region thickness, ρ denotes the pitch between the TSVs, and D_{cnt} is the CNT diameter.

For Cu-CNT composite TSVs, the parasitic capacitance of TSV is determined by the set of capacities in series C_{ox}, C_{dep}, and C_Q. The oxide capacitance and depletion capacitance can be computed using (1) and (2) respectively. C_Q is the quantum capacitance of the CNT forest. This capacitance can be neglected due to its large value compared to the electrostatic one.

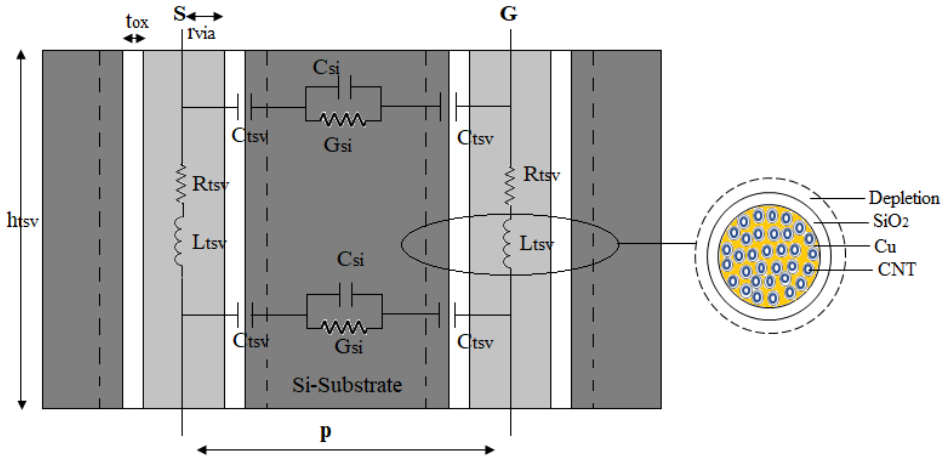

Fig. 2 – *The schematic and equivalent circuit of a pair of Cu-CNT Composite TSVs.*

$$C_{ox} = \frac{\pi \varepsilon_{ox} h_{tsv}}{\ln\left(1 + \frac{t_{ox}}{r_{via}}\right)}, \tag{1}$$

$$C_{dep} = \frac{\pi \varepsilon_{si} h_{tsv}}{\ln\left(1 + \frac{t_{dep}}{r_{via} + t_{ox}}\right)}. \tag{2}$$

The elements of the silicon substrate could be given by:

$$C_{si} = \frac{0.5\pi \varepsilon_{si} h_{tsv}}{\cosh^{-1}\left(\frac{0.5\rho}{r_{via} + t_{ox} + t_{dep}}\right)}, \tag{3}$$

$$G_{si} = \frac{\sigma_{si} C_{si}}{\varepsilon_{si}}, \tag{4}$$

where σ_{si} and ε_{si} are the conductivity and silicon permittivity respectively. σ_{si} depends on temperature, hence, it must be revaluated if the temperature changes using equation of [14], and ρ is the pitch among two TSVs.

The impedance of the TSV is composed of R_{tsv} and L_{tsv}. R_{tsv} presents the internal resistance, which can be obtained using (5). L_{tsv} is the sum of the external inductance among a pair of TSVs (L_{outer}) and the internal inductance (L_{hf}). These two inductances are given by (6) and (7) [14].

$$R_{hf} = \frac{\rho}{2r_{via}} \frac{1}{\sqrt{\left((0.5\rho/r_{via})^2 - 1\right)}} \frac{h_{tsv}}{\pi r_{via} \sigma_{eff} \delta}, \tag{5}$$

$$L_{outer} = \frac{\mu_0 h_{tsv} \cosh^{-1}\left(\frac{0.5\rho}{r_{via}}\right)}{2\pi R_{hf}}, \tag{6}$$

$$L_{hf} = \frac{R_{hf}}{\omega}, \tag{7}$$

where:

$$\sigma_{eff} = (1 - f_{cnt})\sigma_{cu} + f_{cnt}\sigma_{cnt}, \sigma_{cnt} = F_m h_{TSV} \left[\frac{\sqrt{3}}{2}(D_{cnt} + \mathrm{d})^2 Z_{cnt}\right]^{-1}. \tag{8}$$

σ_{cu} is the temperature dependent Cu conductivity, σ_{cnt} is the effective conductivity of CNT forest, and f_{cnt} is the CNT filling ratio. All the parameters in (8) can be calculated using equations of [14]. Equation (8) depends also on F_m, where F_m represents the fraction of metallic CNTs, this various according to multiwalled CNT (MWCNT) and single-walled CNT (SWCNT). Z_{cnt} is the self-intrinsic impedance of isolated CNT, that can be calculated using the equation mentioned in [14], $\mathrm{d} = 0.34[\mathrm{nm}]$.

3 Modelling Coupling Noise of Cu-CNT Composite TSVs

3.1 NILT approach

In the past years, researchers have employed accurate and precise numerical methods in electrical engineering, to address issues related to transients on transmission lines and dynamic systems. One of the most effective techniques used in this context is the Numerical Inverse Laplace Transform (NILT). This was used to ensure inversion accuracy of solutions of fractional order differential equations, and to evaluate their solution transport efficiency. In this study, we have employed a 1D-NILT approach to compute noise coupling in the time domain in 3D structures based on Cu-CNT Composite TSVs.

The 1-dimensional Laplace transform of a function $f(t)$, with $t \geq 0$, is defined as:

$$F(s) = \int_0^\infty f(t)\mathrm{e}^{-st}\,\mathrm{d}t. \tag{9}$$

According to one assumption $\left|f(t)\right| \leq M\,\mathrm{e}^{\alpha t}$, where M is real positive, α is a minimal convergence abscissa, and $F(s)$ is defined on a region

$\{s \in C : \mathrm{Re}[s] \succ \alpha\}$, with $s = c + j\Omega$. c presents the convergence abscissa, $\Omega = 2\pi/\tau$ is a frequency step, and τ presents the solutions region $t \in [0, \tau]$, [24].

Based on the Bromwich integral, the original function can be given [21]:

$$f(t) = \frac{1}{2\pi j} \int_{c-j\infty}^{c+j\infty} F(s) \mathrm{e}^{st} \, \mathrm{d}s \, . \tag{10}$$

Based on a rectangular rule of integration, (11) is found.

$$\tilde{f}(t) = \frac{\mathrm{e}^{ct}}{\tau} \sum_{n=0}^{\infty} F(s) \mathrm{e}^{jn\Omega t} \, . \tag{11}$$

As explained in [22], by substituting $s = c + jn\Omega$ in (9), if the resulting function has integration range divided into an infinite number of steps of the length τ, $F(s)$ is written as:

$$F_n = F(c + jn\Omega) = \sum_{l=0}^{\infty} \int_{l\tau}^{(l+1)\tau} g(t) \, \mathrm{e}^{-jn\Omega t} \, \mathrm{d}t \ , \tag{12}$$

where $g(t)$ is an original exponentially damped function. Afterward, for $t \in [l\tau, \tau(l+1)]$, the functions $g_l(t)$ and $F(s)$ are obtained using (13) and (14):

$$g_l(t) = f(t) \mathrm{e}^{-ct} \, , \tag{13}$$

$$F(c + jn\Omega) = \tau \sum_{l=0}^{\infty} C_{l,n} \, , \tag{14}$$

with:

$$C_{l,n} = \frac{1}{\tau} \int_{l\tau}^{(l+1)\tau} g_l(t) \mathrm{e}^{-jn\Omega t} \, \mathrm{d}t \, . \tag{15}$$

Using complex Fourier series to (13), $g_l(t)$ can be computed by:

$$g_l(t) = \sum_{n=-\infty}^{+\infty} C_{l,n} \, \mathrm{e}^{jn\Omega t} \, . \tag{16}$$

Afterwards, according to (14), (11) and (16), the approximate original function exponentially damped can be expressed as the infinite sum of the newly defined periodic function (13).

Based on (12) – (16), $\tilde{f}(t)$ is got and the absolute error $\varepsilon(t) = \tilde{f}(t) - f(t)$ is computed using (17).

$$\tilde{f}(t) = f(t) + \sum_{l=1}^{\infty} f\left(l\tau + t\right) \mathrm{e}^{-cl\tau} \, . \tag{17}$$

A limited absolute error is determined as $\varepsilon_M(t) \geq \varepsilon(t)$, then $\left| f(t) \right| \leq M\, \mathrm{e}^{\alpha t}$, therefore a limited relative error δ_M can be controlled, and the integration path from the required limited relative error is presented by (18),

$$c = \alpha - \frac{1}{\tau}\ln\left(1 - \frac{1}{1+\delta_M}\right) \approx \alpha - \frac{1}{\tau}\ln\left(\delta_M\right). \tag{18}$$

A suitable technique to speed up the process of achieving the appropriate convergence of series with infinite terms can be represented by (18). This expression is valid with the relative error obtained by the NILT $\tilde{f}(t)$, (17).

Equation (11) can be rewritten based on IFFT and FFT algorithms for efficient computation. Based on the author's experience [21] a quotient-difference (q-d) algorithm of Rutishanser appears to give errors quite close to δ_M predicted by (18) while considering a relatively small number of additional terms.

Considering a discrete variable in the original domain, $t_k = kT$, where T is the sampling period, $\tilde{f}(t)$ could be expressed as follows:

$$\tilde{f}_k = \frac{\mathrm{e}^{ckT}}{\tau} \sum_{n=-\infty}^{\infty} \tilde{F}\left(c + jn\frac{2\pi}{\tau}\right) \exp\left(j2\pi\frac{nkT}{\tau}\right). \tag{19}$$

The formula shown above can be fragmented as:

$$\tilde{f}_k = C_k \left[\sum_{n=0}^{N-1} \tilde{F}^{(-n)} z_{-k}^n + \sum_{n=0}^{\infty} \tilde{G}^{(-n)} z_{-k}^n + \sum_{n=0}^{N-1} \tilde{F}^{(n)} z_k^n + \sum_{n=0}^{\infty} \tilde{G}^{(n)} z_k^n - \tilde{F}^{(0)} \right], \tag{20}$$

with: $\tilde{F}^{(\pm n)} = \tilde{F}(c - jn\Omega)$, $\tilde{G}^{(\pm n)} = \tilde{F}^{(\pm N \pm n)}$, $z_{\pm k} = \exp\left(\pm j\frac{2\pi kT}{\tau}\right)$,

$C_k = \frac{\exp(ckT)}{\tau}$, $N = 2^k$, k is integer, and while $\tau = NT$, $\forall k$, $z_{\pm k}^N = \exp(\pm j2\pi k) = 1$.

The FFT and IFFT algorithms are used to estimate the first and the third part in (20), respectively. The other parts, representing infinite sums, are used as the input data in the q-d algorithm which requires a very small number of additional parameters [23]. The region of calculation should be chosen as: $O_{cal} = (0, t_{cal})$, $t_{cal} = (N/2 - 1)T$.

3.2 *T*-matrix technique:

In order to implement the NILT approach, the frequency domain data of the studied circuit must be computed [18]. Indeed, the *T*-matrix is adopted. The studied circuit and its *T*-matrix illustration are given by Fig. 3. The circuit

depicted in Fig. 3 represents the equivalent circuit of a pair Cu-CNT composite TSVs with terminals. These terminals simulate the Input/Output drivers, a resistor can model the output and a capacitor can present the input driver. The terminals are presented by impedances Z_i, i=1,2,3,4 [24].

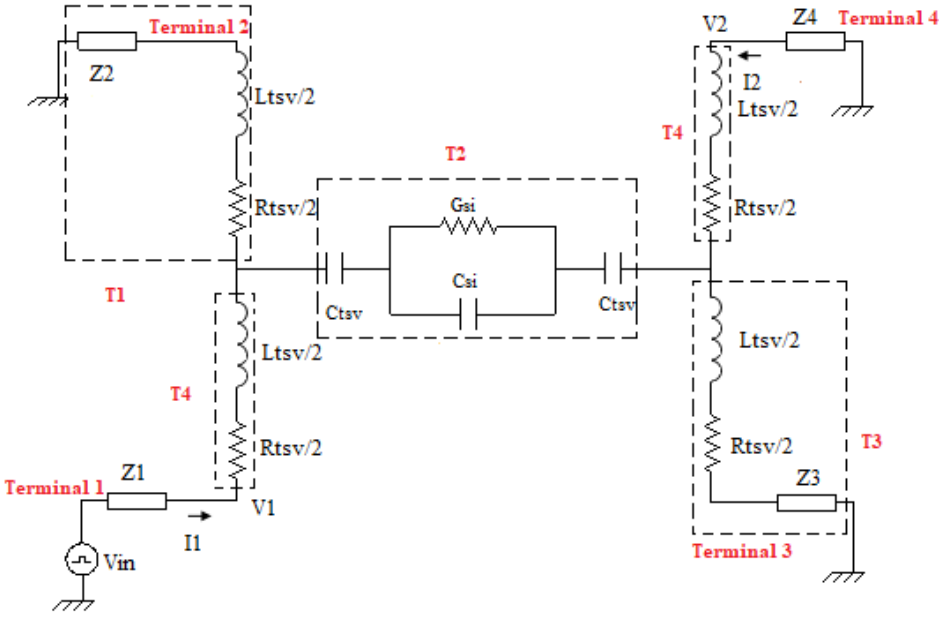

Fig. 3 – *The schematic and equivalent circuit of a pair of Cu-CNT Composite TSVs with terminals.*

The circuit in Fig. 3 is modelled by (21). Its total matrix $\boldsymbol{T}$ is given by (22).

$$\begin{bmatrix} V_1 \\ I_1 \end{bmatrix} = [T] \begin{bmatrix} V_2 \\ -I_2 \end{bmatrix}, \tag{21}$$

$$[T] = [T_4][T_1][T_2][T_3][T_4]. \tag{22}$$

$\boldsymbol{T_1}$, $\boldsymbol{T_2}$, $\boldsymbol{T_3}$, and $\boldsymbol{T_4}$ are given by:

$$[T_1] = \begin{bmatrix} 1 & 0 \\ \dfrac{1}{(R_{tsv}/2 + Z_2 + s L_{tsv}/2)} & 1 \end{bmatrix}, \quad [T_2] = \begin{bmatrix} 1 & Z_{eq} \\ 0 & 1 \end{bmatrix},$$
$$[T_3] = \begin{bmatrix} 1 & 0 \\ \dfrac{1}{(Z_3 + R_{tsv}/2)} & 1 \end{bmatrix}, \quad [T_4] = \begin{bmatrix} 1 & R_{tsv} + sL_{tsv} \\ 0 & 1 \end{bmatrix}, \tag{23}$$

and Z_{eq} is given by:

$$Z_{eq} = \frac{2}{C_{tsv}s} + \frac{R_{si}}{1 + R_{si}C_{si}s}. \tag{24}$$

Based on the previous equations and others from the studied circuit, the coupling presented by V_2 can be computed in the frequency domain using V_{in}. V_{in} is given by (25), where $E(s)$ is a trapezoid, and T is the period of the input signal.

$$V_{in}(s) = \frac{1}{1 - e^{-Ts}} E(s). \tag{25}$$

4 Results and Discussions

Regarding Fig. 3, the time-domain analysis of Cu-CNT composite TSV pair is investigated. The effect of several parameters is studied. It is taken to study a structure with t_{ox} =0.5 µm, r_{via} =2.5 µm, ρ_{tsv} =15 µm, h_{tsv} = 50 µm, t_{dep} = 0.757 µm, and T=300 K. The lumped elements of the circuit of Fig. 3 are computed based on these parameters, and equations (1) – (8).

Because of the miniaturization of 3D structures, the conductivity of Cu is reduced. However, CNTs outperform their Cu. TSVs can be filled with single-walled CNTs (SWCNT), or with multi-walled CNTs (MWCNT), the impacts of these two types of filling are depicted in Fig. 4. In this case, f_{cnt} =1/2, and V_{in} is trapezoidal signal switching from 0 to 1V at 1GHz.

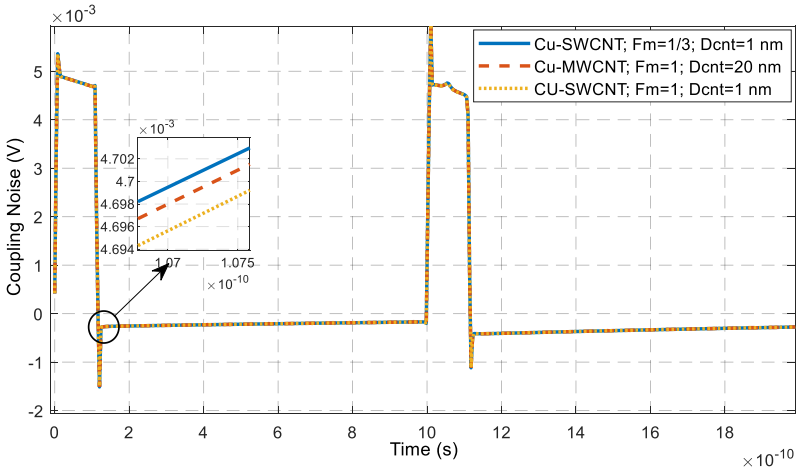

Fig. 4 – *Coupling Noise of Cu-CNT Composite TSVs pair.*

Based on the results depicted in Fig. 4, despite the evolution of 3D structures, the electromagnetic coupling is still observed. The results show that the coupling noise in the three studied cases is similar, it presents a minor difference, as given

by the zoomed part. Observing the zoomed part of the obtained results, with the decrease of the fraction metallic SWCNTs (Fm) in the bundle, the noise is bigger, therefore, the performance of SWCNT-TSV is degraded.

The impact of different geometrical parameters on the coupling noise of Cu-CNT composite TSVs is examined, as depicted in Figs. 5 – 8. It is found that with the increase of oxide thickness (Fig. 5), the coupling noise increases in the transition area and decreases when the state of the input changes. Generally, the performance of the structure can be improved with the increase of oxide thickness, because of the increased TSV capacitance, especially at high frequencies. Based on the results, it is found that varying the CNT filling ratio (f_{cnt}) has no impact on the coupling noise in the time domain (Fig. 6). However, the pitch between TSVs must also be considered. Fig. 7 demonstrates that as the pitch increases the coupling noise in time domain decreases. This is due to the decrease in both silicon capacitance and conductance. At high frequencies, the effect of silicon capacitance becomes dominant, resulting in increased coupling noise the coupling noise, and worsened insertion loss.

Furth more, the temperature can influence on the coupling noise, therefore, it is examined. At high frequencies (>10 GHz), the silicon substrate can be considered as a pure dielectric, where the dielectric loss is important. The dielectric loss decreases when T increases. Consequently, the magnitude of the coupling noise increases at low frequencies and decreases at high frequencies. In this study, the elements of the studied circuit have been calculated at frequencies lower than 10 GHz. This is why it is observed in Fig. 8 that, when the temperature increases, the noise decreases. This is due to a decrease in TSV capacitance.

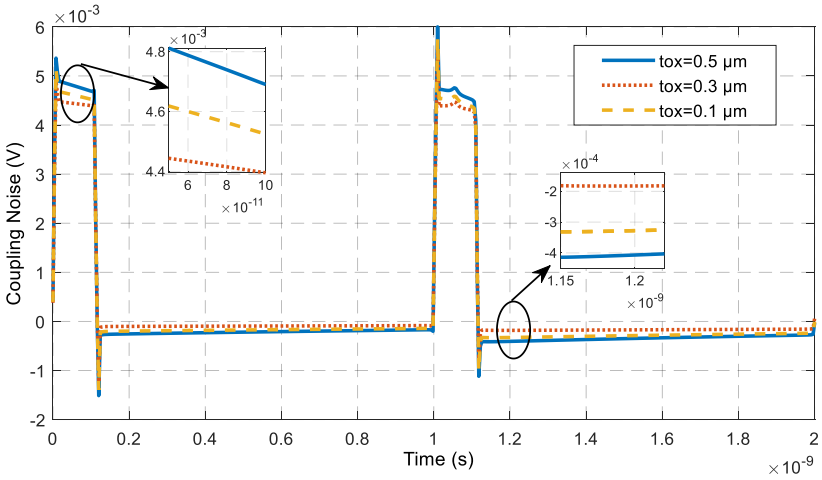

Fig. 5 – *Coupling Noise of Cu-CNT Composite TSVs pair with different* t_{ox}.

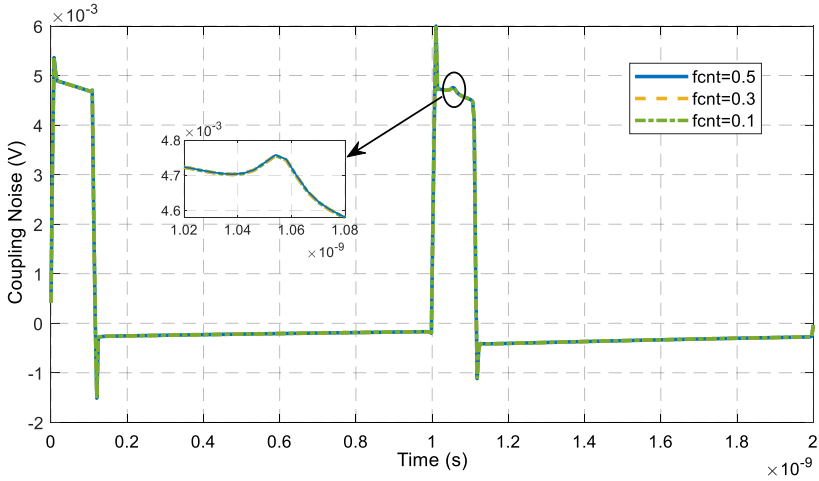

Fig. 6 – *Coupling Noise of Cu-CNT Composite TSVs pair with different CNT filling ratio.*

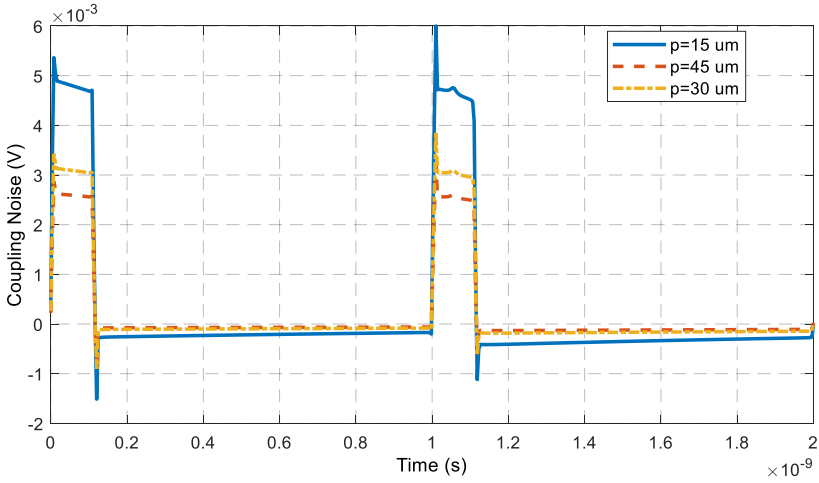

Fig. 7 – *Coupling Noise of Cu-CNT Composite TSVs pair with different pitch.*

Based on the results obtained in this study and those reported in [24], it can be seen that the coupling noise in structures based on Cu-CNT is lower compared to structures based on Cu-TSV especially at high frequencies. Otherwise, in some references in literature [25], it was concluded that the graphene nanoribbons (GNRs) are more appropriate as an interconnect material for fabricating advanced electronic circuits and devices.

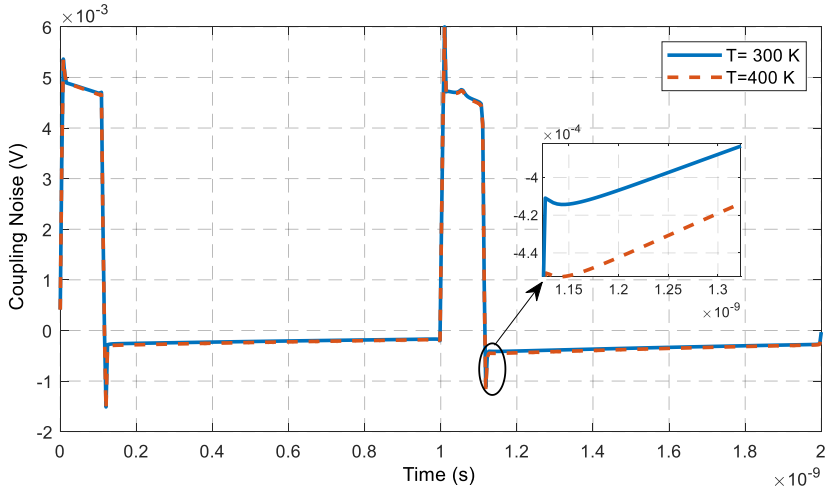

Fig. 8 – *Coupling Noise of Cu-CNT Composite TSVs pair with different temperature.*

5 Conclusions

In this paper, a theoretical technique was proposed to compute the coupling noise of equivalent-circuit model of Cu-CNT composite TSVs, in the time domain. The main objective of the study was to investigate the characteristics of this type of noise in high-speed 3D-ICs. The proposed method was based on *T*-matrix and NILT. Based on the proposed method and the equivalent circuit, the characteristics of coupling noise of Cu-CNT composite TSVs were conscious. It is found that the coupling noise can be impacted by the type of filling, geometrical and physical parameters. It is also found that the coupling noise can be important and can even influence the normal operation of a 3D electronic systems, indeed coupling reduction techniques such as adding repeaters are necessary. As a result, our next work will be on coupling reduction.

6 References

[1] I. Ndip, B. Curran, K. Lobbicke, S. Guttowski, H. Reichl, K.- D. Lang, H. Henke: High-Frequency Modeling of TSVs for 3-D Chip Integration and Silicon Interposers Considering Skin-Effect, Dielectric Quasi-TEM and Slow-Wave Models, IEEE Transactions on Components, Packaging and Manufacturing Technology, Vol. 1, No. 10, October 2011, pp. 1627 – 1641.

[2] Z. Xu, J.- Q. Lu: Through-Strata-Via (TSV) Parasitics and Wideband Modeling for Three-Dimensional Integration/Packaging, IEEE Electron Device Letters, Vol. 32, No. 9, September 2011, pp. 1278 – 1280.

[3] L. Qian, Y. Xia, G. Liang: Study on Crosstalk Characteristic of Carbon Nanotube Through Silicon Vias for Three Dimensional Integration, Microelectronics Journal, Vol. 46, No. 7, July 2015, pp. 572 – 580.

[4] E.- X. Liu, E.- P. Li, W.- B. Ewe, H. M. Lee, T. G. Lim, S. Gao: Compact Wideband Equivalent-Circuit Model for Electrical Modeling of Through-Silicon Via, IEEE Transactions on Microwave Theory and Techniques, Vol. 59, No. 6, June 2011, pp. 1454 – 1460.

[5] J. Kim, J. S. Pak, J. Cho, E. Song, J. Cho, H. Kim, T. Song, J. Lee, H. Lee, K. Park, S. Yang, M.- S. Suh, K.- Y. Byun, J. Kim: High-Frequency Scalable Electrical Model and Analysis of a Through Silicon Via (TSV), IEEE Transactions on Components, Packaging and Manufacturing Technology, Vol. 1, No. 2, February 2011, pp. 181 – 195.

[6] B. K. Kaushik, M. K. Majumder, V. R. Kumar: Carbon Nanotube Based 3-D Interconnects - A Reality or a Distant Dream, IEEE Circuits and Systems Magazine, Vol. 14, No. 4, Fourthquarter 2014, pp. 16 – 35.

[7] V. R. Kumar, B. K. Kaushik, A. Patnaik: Crosstalk Noise Modeling of Multiwall Carbon Nanotube (MWCNT) Interconnects Using Finite-Difference Time-Domain (FDTD) Technique, Microelectronics Reliability, Vol. 55, No. 1, January 2015, pp. 155 – 163.

[8] V. R. Kumar, B. K. Kaushik, M. K. Majumder: Graphene Based On-Chip Interconnects and TSVs: Prospects and Challenges, IEEE Nanotechnology Magazine, Vol. 8, No. 4, December 2014, pp. 14 – 20.

[9] W.- Sh. Zhao, W.- Y. Yin: Carbon-Based Interconnects for RF Nano-Electronics, Wiley Encyclopedia of Electrical and Electronics Engineering, John Wiley & Sons, Inc., Hoboken, 2012.

[10] T. Wang, S. Chen, D. Jiang, Y. Fu, K. Jeppson, L. Ye, J. Liu: Through-Silicon Vias Filled with Densified and Transferred Carbon Nanotube Forests, IEEE Electron Device Letters, Vol. 33, No. 3, March 2012, pp. 420 – 422.

[11] G.- F. Wang, W.- S. Zhao, L.- L. Sun: Overview of Carbon-Based Passives, Acta Electronica Sinica, Vol. 45, No. 12, December 2017, pp. 3037-3045. (in Chinese)

[12] W.- S. Zhao, W.- Y. Yin, Y.- X. Guo: Electromagnetic Compatibility-Oriented Study on Through Silicon Single-Walled Carbon Nanotube Bundle Via (TS-SWCNTBV) Arrays, IEEE Transactions on Electromagnetic Compatibility, Vol. 54, No. 1, February 2012, pp. 149 – 157.

[13] W.- S. Zhao, L. Sun, W.- Y. Yin, Y.- X. Guo: Electrothermal Modeling and Characterization of Submicron Through-Silicon Carbon Nanotube Bundle Vias for Three-Dimensional ICs, Micro & Nano Letters, Vol. 9, No. 2, February 2014, pp. 123 – 126.

[14] L. Qian, Z. Zhu, Y. Xia: Study on Transmission Characteristics of Carbon Nanotube Through Silicon via Interconnect, IEEE Microwave and Wireless Components Letters, Vol. 24, No. 12, December 2014, pp. 830 – 832.

[15] Y. Chai, P. C. H. Chan, Y. Fu, Y. C. Chuang, C. Y. Liu: Electromigration Studies of Cu/Carbon Nanotube Composite Interconnects Using Blech Structure, IEEE Electron Device Letters, Vol. 29, No. 9, September 2008, pp. 1001 – 1003.

[16] Y. Chai, P. C. H. Chan, Y. Fu, Y. C. Chuang, C. Y. Liu: Copper/Carbon Nanotube Composite Interconnect for Enhanced Electromigration Resistance, Proceedings of the 58th Electronic Components and Technology Conference, Lake Buena Vista, USA, May 2008, pp. 412 – 420.

[17] V. R. Kumar, B. K. Kaushik, A. Patnaik: An Accurate Model for Dynamic Crosstalk Analysis of CMOS Gate Driven On-Chip Interconnects Using FDTD Method, Microelectronics Journal, Vol. 45, No. 4, April 2014, pp. 441 – 448.

[18] V. R. Kumar, A. Alam, B. K. Kaushik, A. Patnaik: An Unconditionally Stable FDTD Model for Crosstalk Analysis of VLSI Interconnects, IEEE Transactions on Components, Packaging and Manufacturing Technology, Vol. 5, No. 12, December 2015, pp. 1810 – 1817.

[19] K. G. Verma, B. K. Kaushik, R. Singh: Effects of Process Variation in VLSI Interconnects – A Technical Review, Microelectronics International, Vol. 26, No. 3, 2009, pp. 49 – 55.

[20] K. Fu, J. Zheng, W. Sh. Zhao, Y. Hu, G. Wang: Analysis of Transmission Characteristics of Copper/Carbon Nanotube Composite Through-Silicon Via Interconnects, Chinese Journal of Electronics, Vol. 28, No. 5, September 2019, pp. 920 – 924.

[21] N. Al-Zubaidi Smith, L. Brančík: Convergence Acceleration Techniques for Proposed Numerical Inverse Laplace Transform Method, Proceedings of the 24th Telecommunication Forum (TELFOR), Belgrade, Serbia, November 2016, pp. 1 – 4.

[22] L. Brancik: Numerical Inversion of Two-Dimensional Laplace Transforms Based on Partial Inversions, Proceedings of the 17th International Conference Radioelektronika, Brno, Czech Republic, April 2007, pp. 1 – 4.

[23] Y. Shim, J. Park, J. Kim, E. Song, J. Yoo, J. Pak, J. Kim: Modeling and Analysis of Simultaneous Switching Noise Coupling for a CMOS Negative-Feedback Operational Amplifier in System-in-Package, IEEE Transactions on Electromagnetic Compatibility, Vol. 51, No. 3, August 2009, pp. 763 – 773.

[24] K. Ait Belaid, H. Belahrach, H. Ayad: Numerical Laplace Inversion Method for Through-Silicon Via (TSV) Noise Coupling in 3D-IC Design, Electronics, Vol. 8, No. 9, September 2019, p. 1010.

[25] A. Hazra, S. Basu: Graphene Nanoribbon as Potential On-Chip Interconnect Material – A Review, C – Journal of Carbon Research, Vol. 4, No. 3, August 2018, p. 49.